Nonlinear model predictive control applied to multivariable thermal and chemical control of selective catalytic reduction aftertreatment

Sowman, J., Laila, D. S., Fussey, P., Truscott, A. & Cruden, A.

Author post-print (accepted) deposited by Coventry University's Repository

Original citation & hyperlink:
Sowman, J, Laila, DS, Fussey, P, Truscott, A & Cruden, A 2019, 'Nonlinear model predictive control applied to multivariable thermal and chemical control of selective catalytic reduction aftertreatment', International Journal of Engine Research, vol. (In-press), pp. (In-press).
https://dx.doi.org/10.1177/1468087419859103

DOI 10.1177/1468087419859103
ISSN 1468-0874
ESSN 2041-3149

Publisher: SAGE Publications

Copyright © and Moral Rights are retained by the author(s) and/ or other copyright owners. A copy can be downloaded for personal non-commercial research or study, without prior permission or charge. This item cannot be reproduced or quoted extensively from without first obtaining permission in writing from the copyright holder(s). The content must not be changed in any way or sold commercially in any format or medium without the formal permission of the copyright holders.

This document is the author's post-print version, incorporating any revisions agreed during the peer-review process. Some differences between the published version and this version may remain and you are advised to consult the published version if you wish to cite from it.

Journal Title
XX(X):1–7
©The Author(s) 2016
Reprints and permission:
sagepub.co.uk/journalsPermissions.nav
DOI: 10.1177/ToBeAssigned
www.sagepub.com/
SAGE

Nonlinear MPC Applied to Multivariable Thermal and Chemical Control of SCR Aftertreatment

Jonathan Sowman[1], Dina Shona Laila[2], Peter Fussey[3], Anthony Truscott[3] and Andrew J. Cruden[4]

Abstract

Manufacturers of diesel engines are under increasing pressure to meet progressively stricter NO_x emissions limits. A key NO_x abatement technology is selective catalytic reduction (SCR) in which ammonia, aided by a catalyst, reacts with NO_x in the exhaust stream to produce nitrogen and water. The conversion efficiency is temperature dependent: at low temperature, reaction rates are temperature limited, resulting in suboptimal NO_x removal, whereas at high temperatures, they are mass transfer limited. Maintaining sufficiently high temperature to allow maximal conversion is a challenge, particularly after cold start, as well as during conditions in which exhaust heat is insufficient, such as periods of low load or idling. In this work, a nonlinear model predictive controller simultaneously manages urea injection and power to an electric catalyst heater, in the presence of constraints.

Keywords

Model Predictive Control, Selective Catalytic Reduction, Diesel Aftertreatment Controls

Introduction

Concentrations of oxides of nitrogen (NO_x) are a topical issue in many urban environments across the world. Nitrogen dioxide (NO_2) is responsible for various diseases and physiological disorders such as decrements lung function and lung function growth, increases in symptoms of respiratory problems, asthma prevalence and incidence, cancer incidence and adverse birth outcomes and mortality[1]. Heavy duty diesel engines are notorious for their emission of these pollutants.

The most promising after-treatment technologies for removal of NO_x in heavy duty applications is selective catalytic reduction (SCR) and Lean NOx-Trap (LNT)[2–4]. In this paper, we focus on the SCR technology. This chemical system operates by injection of a urea solution before a catalyst, which is hydrolysed into gaseous ammonia. This ammonia adsorbs onto the catalytic surface, after which it reacts with NO_x to produce nitrogen and water. Being a chemical system, the reaction rates are highly temperature dependent[5]. Where possible, avoidance of heavy duty diesel engines operating in city centre environments is to be encouraged. However, public buses, delivery vehicles and plant equipment are examples of where this is often impossible. Combined with urban traffic, low engine speeds and engine mass flow rates result in catalyst cooling, whereupon removal of NO_x from the exhaust gas stream is suboptimal.

Industry standard approaches for automotive control have typically been the basis of SCR control, which are typically feedforward map-based controllers whose maps are calibrated on the testbed over test cycles during engine development. There has been speculation that closed-loop control will be required in the future to cope with the combination of stricter emissions requirements, highly transient plant operation, and variation in sensors and actuators both during production and over the life cycle of the aftertreatment system[6]. As a result, elements of feedback control have begun to make their way into industry standard SCR controllers, including Proportional Integral (PI)[7–9] and sliding mode[10,11]. The calibration effort required to tune a map-based controller is extensive, and constraints cannot be enforced in a systematic manner. The response of a linear controller (such as PI) means that steady states must typically be placed further from constraint boundaries to achieve sufficiently low probability of constraint violation. All of these reasons comprise the motivation for exploring model-based control for SCR.

A significant feature of emission control is the requirement to follow a set of limits of the level of the emission gasses. For this reason, model predictive control (MPC) have shown significant promise when applied to SCR[12–14]. Their natural handling of constraints and transport delays incurred in the chemical SCR system permit operation the SCR plant closer to optimal conditions. This results in improved performance in all respects: NO_x removal, ammonia slip, and consumption of urea solution. In this work, we examine the possibility of extended the MPC controller to include thermal management of SCR. This has been attempted in the

[1]Frazer-Nash Consultancy Ltd, UK
[2]School of Mechanical, Aerospace and Automotive Engineering, Coventry University, UK
[3]Ricardo UK Ltd, Shoreham-by-Sea, UK
[4]Energy Technology Group, Faculty of Engineering and the Environment, University of Southampton, UK

Corresponding author:
Dina Shona Laila, Coventry University, UK.
Email: dina.laila@coventry.ac.uk

literature using post-injection of fuel to elevate the exhaust gas temperature[15].

In this work, we employ an electric catalyst heater to compensate low gas temperature. This is preferable to post-injection for two reasons: ease of retrofitting, which is required in the case of large vehicle fleets, and possibility to use recovered energy from hybridisation technology. We leverage the natural ability of MPC to be extended to multiple-input multiple-output (MIMO) problems. New vehicles conforming to the Euro VI standard (since January 2014) demonstrate up to 95% less NO_x emissions compared to Euro V. However, the turnover of large vehicle fleets is such that retrofitting of after-treatment systems is currently being examined as the preferred option to bring the fleet up to modern emissions standards[16].

The nonlinear MPC controller designed in this study is applied to the SCR model which is constructed based on data obtained from a test bed measurement using a Ricardo 2.0 litre turbocharged and inter-cooled diesel engine, with the SCR installed on the exhaust line. Simulation results are presented and discussed, comparing the closed-loop performance of the SCR system with and without the heater.

Review of Selective Catalytic Reduction

Selective catalytic reduction (SCR) is an actively controlled chemical process which converts NO_x into nitrogen and water. A diagram of the SCR catalyst is shown in Figure 1. The key reactant is ammonia, which is delivered into the exhaust stream in the form of an aqueous solution, which then hydrolyses to ammonia due to the heat of the exhaust:

$$CH_4N_2O + H_2O2NH_3 + CO_2. \tag{1}$$

It is necessary that ammonia in the free stream adsorbs onto the catalyst washcoat, since the SCR reactions take place between gaseous NO_x and adsorbed ammonia. The storage of ammonia is an equilibrium reaction:

$$NH_3 \Longleftrightarrow NH_3^*, \tag{2}$$

where * indicates a species existing on the catalytic surface. The double arrow in this reaction indicates that ammonia can leave the catalyst surface and return to the free stream, if the diffusion gradient favours such movement. This desorption is a process which the control systems must aim to minimise, as it implies unreacted ammonia exiting the tailpipe, known as ammonia slip. The adsorbed ammonia is now available to participate in the SCR reactions that comprise:

1. the *standard SCR* reaction

$$4NH_3^* + 4NO + O_2 \Longrightarrow 4N_2 + 6H_2O, \tag{3}$$

2. and the *fast SCR* reaction

$$2NH_3^* + NO + NO_2 \Longrightarrow 2N_2 + 3H_2O, \tag{4}$$

where the former reduces only NO and the latter consumes equal quantities of NO and NO_2.

The SCR catalyst has a characteristic light-off temperature, which marks the temperature boundary between temperature-limited reaction rates and mass transfer limited

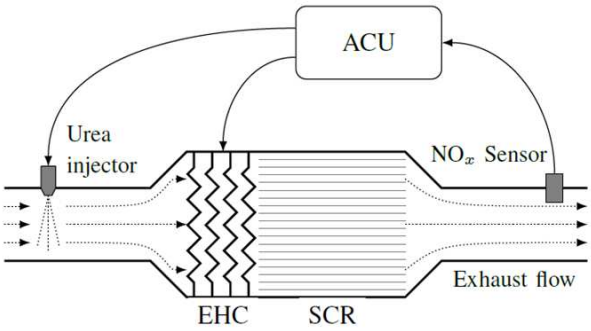

Figure 1. Schematic of an SCR catalyst fitted with an electric catalyst heater (EHC). Also shown is the aftertreatment control unit (ACU).

reactions. The rates for the standard and fast SCR are given by Arrhenius expressions:

$$r_I = A_i \exp\left(\frac{-B_i}{RT_{mon}}\right), \tag{5}$$

where A_i and B_i are constants to be determined for each reaction, R is the universal gas constant and T_{mon} is the temperature of the catalyst monolith. The catalytic washcoat has an ammonia storage capacity which is a material property, and is the maximum possible stored ammonia per unit volume, denoted ψ. In operation, this maximum storage is not achieved, since the reaction rates determine the storage level[17]. For adsorption, the reaction rate is given by:

$$r_{ads} = k_{ads}^0 C_{NH_3}(1-\theta), \tag{6}$$

whilst that for desorption is given by

$$r_{des} = k_{des}^0 \exp\left(-\frac{B_{des}}{RT_{mon}}(1-\alpha\theta)\right)\theta, \tag{7}$$

where k_{ads}, k_{des}, and B_{des} are calibration constants, C_{NH_3} is the gas concentration of ammonia in the catalyst and θ is defined as the ratio of the current storage per unit volume to the materially determined maximum:

$$\theta = \frac{\psi}{\Phi}, \tag{8}$$

where Φ is the maximum ammonia storage of the catalyst in kmol/m^3.

Thermal Management

Due to minimal interaction with the engine fuelling control loop, electric catalyst heaters are a likely candidate for retrofitting to existing diesel vehicles fitted with SCR whose NO_x conversion performance is lower than ideal. An electrically heated catalyst (EHC) is modelled as a gas heater attached to the front face of the catalyst monolith, as shown in Figure 1. We model this heater as being close-coupled with the catalyst in order to maximise the heat transfer between the heater elements and the catalyst monolith. The monolith is not heated directly as this leads to localised hot spots which can damage the catalyst – instead, the exhaust gas is

heated before it enters the SCR brick. A particular heater was selected which has a maximum power of 3.6 kilowatts at 12 Volts. The model of the heater is a simple energy balance given by:

$$\delta T_{heater} = \frac{P_{heater}}{\dot{m} c_p}, \tag{9}$$

where P_{heater} is the electrical power supplied to the heater, $\dot{m}$ is the mass flow rate of exhaust gas, and c_p is the specific heat of the exhaust gas (at constant pressure). A pair of thermocouples in the SCR catalyst enclosure monitor the gas temperatures before and after the monolith. Monitoring the SCR monolith temperature directly is difficult due to sensor embedding, so we infer this via the gas temperature sensors.

Control Oriented SCR Modelling

We use the continuously stirred tank reactor model:

$$\dot{N}(t) = F_{in}(t) - F_{out}(t) + V v_i r_i(t), \tag{10}$$

where F_{in} and F_{out} are the molar flow rates of the species in and out of the reactor respectively, V is the reactor volume, v_i and r_i are the stoichiometric coefficient and reaction rate of species i respectively. Since reaction rates are functions of the monolith temperature T_{mon}, whereas only the upstream exhaust temperature $T_{exh,in}$ is measured, as in[2,3] a simple first order thermal model is utilised, which is

$$\begin{aligned}\frac{d}{dt}T_{mon} =& k_M \left(T_{exh,in} + \Delta T_{heater} - T_{mon}\right) \\ &+ k_A (T_{mon} - T_{amb}).\end{aligned} \tag{11}$$

The heat release from the chemical kinetics is neglected in this model. The parameter k_M models the convectional heat transfer from the exhaust gases to the monolith, whilst the parameter k_A models heat loss from the monolith to the environment at temperature T_{amb}. These two parameters include the information of the mass and specific heat of the monolith:

$$k_M = \frac{qnC_{exh}}{m_{mon}C_{mon}}, \qquad k_A = \frac{\varepsilon_{rad}\sigma_{rad}A_{rad}}{m_{mon}C_{mon}}$$

with q the mass flow rate of the exhaust gas, n the number of the SCR cells, C_{exh} the specific heat at constant pressure of the exhaust gas, ε_{rad} the radiation coefficient of the silencer, σ_{rad} the radiation constant, A_{rad} the radiation surface, m_{mon} the mass of the monolith and C_{mon} the specific heat of the monolith.

Grouping the NO_x and ammonia gas concentrations and the monolith temperature, we get a 4-state model with state vector:

$$x := \begin{bmatrix} C_{NO_x}, & \psi, & C_{NH_3}, & T_{mon} \end{bmatrix}^T \tag{12}$$

control inputs vector:

$$u := \begin{bmatrix} NH_{3,inj}, & P_{heater} \end{bmatrix}^T, \tag{13}$$

and the disturbance input vector:

$$d := \begin{bmatrix} NO_{x,in}, & T_{exh,in} \end{bmatrix}^T. \tag{14}$$

The resulting model can be written in nonlinear state-space form as

$$\begin{aligned}\begin{bmatrix} \dot{C}_{NO_x} \\ \dot{\psi} \\ \dot{C}_{NH_3} \\ \dot{T}_{mon} \end{bmatrix} =& \begin{bmatrix} 0 & 0 \\ 0 & 0 \\ \frac{1}{V} & 0 \\ 0 & \frac{k_M}{c_p \dot{m}} \end{bmatrix} u(t) + \begin{bmatrix} \frac{1}{V} & 0 \\ 0 & 0 \\ 0 & 0 \\ 0 & k_M \end{bmatrix} d(t) \\ &+ \begin{bmatrix} \psi R_{oxi} - C_{NO_x}(\psi R_{red} + F) \\ R_{ads}C_{NH_3}\Phi - \psi(R_{ads}C_{NH_3} + R_{des} + R_{red}C_{NO_x} + R_{oxi}) \\ \psi R_{des} - C_{NH_3}(R_{ads}(\Phi - \psi) + F) \\ -k_M T_{mon} - k_A(T_{mon} - T_{amb}) \end{bmatrix}.\end{aligned} \tag{15}$$

Nonlinear Model Predictive Control

Begin with the control oriented dynamic model of the system (15) expressed in the form

$$\dot{x} = f\left(x(t), u(t), d(t)\right), \tag{16}$$

As we do not consider robustness property in the control design, we assume the disturbances as constant throughout the design, thus we can write the model as

$$\dot{x} = f\left(x(t), u(t)\right), \tag{17}$$

with constraints on the states $x \in X$ and inputs $u \in U$. The time arguments of x and u are included to emphasise that f depends on time only via the states and inputs (i.e., the model is time invariant). Then, model predictive control (MPC) attempts to find a solution trajectory $u^\star(t)$ over a finite time horizon H_p. It attempts to choose this trajectory such that:

1. It is constraint admissible, such that the states and inputs remain in their respective sets of constraints.
2. It is optimal against some predefined cost function.

The superscript * is used to denote that a quantity is optimal with respect to the cost function. Given that the prediction horizon is divided into N time steps, a typical cost function for MPC is usually written in the form:

$$J(x(t), u(t)) = \int_{t_0}^{t_0+H_p} l(x(t), u(t))\mathrm{d}t + E(x(t_0 + H_p)), \tag{18}$$

where $l(\cdot,\cdot)$ is the *stage cost* and $E(\cdot)$ is the *terminal cost*. The terminal cost is usually included to prove stability of the closed-loop feedback scheme. However, we do not consider such proofs in this work and as such, it is neglected. For the stage cost, we choose a least-squares form:

$$l(x, u) = \|x - x_{ref}\|_Q^2 + \|u - u_{ref}\|_R^2, \tag{19}$$

in which x_{ref} and u_{ref} are predefined reference trajectories for the states and inputs, and Q and R are weighting matrices which are to be tuned in order to prioritise tracking of particular states and inputs over others. Using this notation, we can write the nonlinear MPC problem as follows:

$$\begin{aligned} \underset{u}{\text{minimise}} \quad & J(x, u) && \text{(20a)} \\ \text{subject to} \quad & \dot{x} = f(x, u) && \text{(20b)} \\ & u \in U \;\forall\; t \in [t_0, t_0 + H_p] && \text{(20c)} \\ & x \in X \;\forall\; t \in [t_0, t_0 + H_p] && \text{(20d)} \\ & x_0 = \tilde{x}_0, && \text{(20e)} \end{aligned}$$

where $\tilde{x}_0$ is the measured state of the plant at time t_0. Equation (20) is called the finite horizon optimal control problem (FHOCP) and its numerical solution is the subject of significant current research into real-time application of nonlinear MPC.

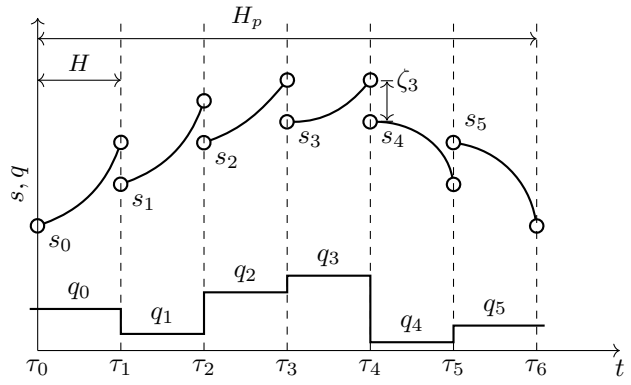

Figure 2. Depiction of direct multiple shooting with $N = 6$. With s_k and q_k we denote the initial state and piecewise constant controls in each segment k. The defects in each segment ζ_k are forced to 0 by the optimisation programme.

One method which has seen success in various arenas of applied optimal control is direct multiple shooting (DMS). In this scheme, the prediction horizon is discretised into N segments each of duration H, such that $N := \frac{H_p}{H}$. To distinguish between real and predicted states and inputs, predicted states and inputs at time k are denoted with s_k and q_k respectively. The inputs q_k are assumed to be constant over each discretisation node, as shown in Figure 2. Note that variables ζ_k are introduced such that they can be forced to 0 in the optimisation programme, thereby ensuring consistency in the state trajectories. Then, grouping the state and input in each segment as

$$z_n := \begin{bmatrix} s_n, & q_n \end{bmatrix}^T, \; \forall \, n \in \{0, \ldots, N-1\}, \tag{21}$$

we try and find the optimum of z, which is defined as:

$$z := \begin{bmatrix} z_0^T, & z_1^T, & \ldots, & z_{N-1}^T, & s_N \end{bmatrix}^T. \tag{22}$$

This formulation allows us to write a nonlinear optimisation problem (NLP):

$$\begin{aligned}
\underset{z}{\text{minimise}} \quad & \sum_{n=0}^{N-1} l(z_n) + E(s_N) && \text{(23a)}\\
\text{subject to} \quad & s_0 = x_0 && \text{(23b)}\\
& \zeta_n = s_{n+1} - F(z_n) = 0 && \text{(23c)}\\
& g(z) = 0 && \text{(23d)}\\
& h(z) \leq 0, && \text{(23e)}
\end{aligned}$$

where F denotes the solution at time $n+1$ of the initial value problem given by the model (17) at time n, and g and h contain the equality and inequality constraints respectively.

In this work, we solve this problem using a real-time iterations strategy[18]. The least-squares cost chosen for (19) allows us to leverage the Gauss-Newton Hessian approximation which eases computation further. This is a sequential quadratic programming (SQP) approach in which one quadratic programme (QP) is solved for each real timestep of the plant. This approach aims to minimise the delay between receiving the measurement of the plant state and applying the control $u^\star$, by separation of the SQP algorithm into *preparation* and *feedback* stages. During preparation, the model equations are evaluated with a predicted state measurement; this is the most time consuming part of the algorithm. This means most of the QP matrices can be constructed before the measurement arrives, leaving few calculations, as well as the solution of the QP, to be executed in the feedback phase. To hasten solution of the QPs, the qpOASES package[19] is employed in this work. Since it solves QPs in a multiparametric manner, solutions can be generated very quickly with knowledge of the optimum at the previous time step.

Results

In this study, the nonlinear model predictive control strategy is applied to the SCR model (15). Data are obtained from a test bed measurement using a Ricardo 2.0 litre turbocharged and inter-cooled diesel engine, with the SCR installed on the exhaust line.

Given the plant model, we choose a prediction horizon $H_p = 20$ seconds, with a DMS step size $H = 1$ second. This ensures that a significant portion of the slowest dynamics (the monolith temperature) is captured during the prediction horizon such that the optimisation can make a judicious choice of heater power.

Referring to equation (13), the control inputs in this case are the amount of NH_3 injected to the SCR catalyst chamber, NH_3, inj, and the electrical power supplied to the heater, P_{heater}. These inputs are constrained to

$$10^{-12} \leq NH_{3,inj} \leq 5 \times 10^{-5} \text{ kmol/s} \tag{24a}$$

$$10^{-12} \leq P_{heater} \leq 5 \times 3600 \text{ Watts} \tag{24b}$$

where the lower limits are chosen for the sake of good numerical conditioning of the model, and the upper limits are determined by the physical actuators. Preferred reference state and input trajectories x_{ref} and u_{ref} are not generally known a priori. As such, $x_{ref} = u_{ref} = 0$, with the exception of the reference for the monolith temperature whose reference is set to $250°$C.

Choosing Q and R in (19) is vital in assuring good performance of the controller. In the results presented in this section, we choose:

$$Q = \begin{bmatrix} 10^3 & 0 & 0 & 0 \\ 0 & 10^{-12} & 0 & 0 \\ 0 & 0 & 10^2 & 0 \\ 0 & 0 & 0 & 10^3 \end{bmatrix} \tag{25}$$

The very small value of the element $q_{2,2}$ which is the weight on ψ, is chosen because the quantity of ammonia stored in the SCR is not a concern from an emissions perspective; instead we choose to weight the NO_x and NH_3 tailpipe emissions. We also weight the monolith temperature T_{mon} since we prefer that the monolith temperature remains near its reference, as we have the dual objective in this case of maximising catalyst efficiency whilst not ensuring it does not overheat.

Table 1. Effect of varying electric catalyst heater penalty on SCR efficiency.

Weight	SCR Efficiency (%)	Energy (Wh)
10^{-3}	67.2	201
10^{-2}	66.5	190
10^{-1}	58.9	123
10^{0}	45.6	27

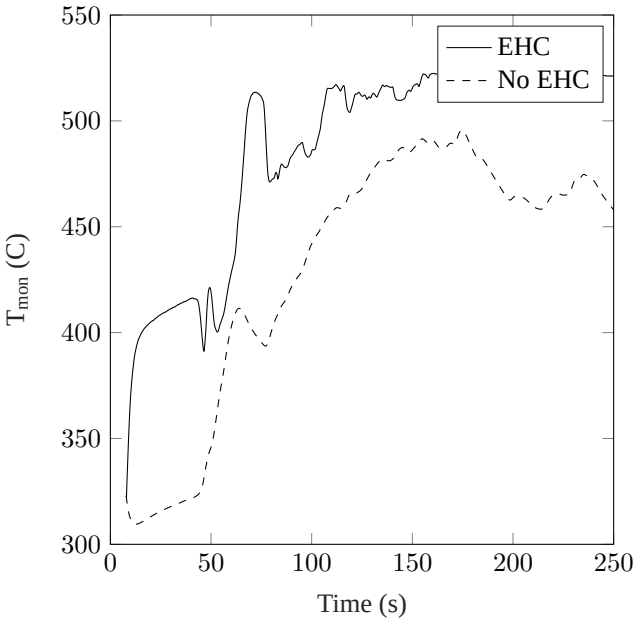

Figure 3. Catalyst monolith temperature with and without the catalyst heater.

For the input weights, we choose:

$$R = \begin{bmatrix} 10^{-1} & 0 \\ 0 & 10^{-2} \end{bmatrix} \tag{26}$$

since whilst the primary objectives are minimisation of tailpipe NO_x and ammonia, it is preferable to minimise urea consumption and catalyst heater power when they are not limiting to SCR efficiency. Choosing the weights for Q and R imply a structured objective: use the minimum possible urea and heater energy whilst adhering to the principle objective of maximising NO_x removal from the exhaust stream. This is done whilst respective the imposed constraints.

The controller was tested on the first 250 seconds of a cold-start NRTC cycle using input data acquired on a testbed. The results for varying weights of the heater input are shown in Table 1. Enabling the catalyst heater in the MPC controller raises the temperature of the catalyst monolith significantly faster than relying solely on heat in the exhaust gas stream, as can be seen in Figure 3. Since a cold start is occurring, the controller opts to enable the heater at maximum power (3.6 kW) for the first part of the cycle, as shown in Figure 4. The result of this is raising of the SCR monolith temperature significantly faster than when the catalyst heater is not used, as shown in Figure 5.

Higher catalyst temperatures enable the increase of the SCR reaction rates, which are limiting to NO_x conversion in this temperature region. The result is that, as shown in Figure 5, the quantity of NO_x emitted from the tailpipe is significantly reduced. In fact, over this portion of the cold-start test cycle, the cumulative NO_x emitted is reduced by 39%. The NH_3 consumption, which in this case is the control input to the system, also increases as soon as the heating element is enabled, as the higher temperature allows more NH_3 to take part in the SCR reactions. As can be seen in Figure 6, this also causes higher level of ammonia slips at the beginning of the cycle. However, as the temperature is stabilizing, the ammonia slip gets lower which implies a more efficient control.

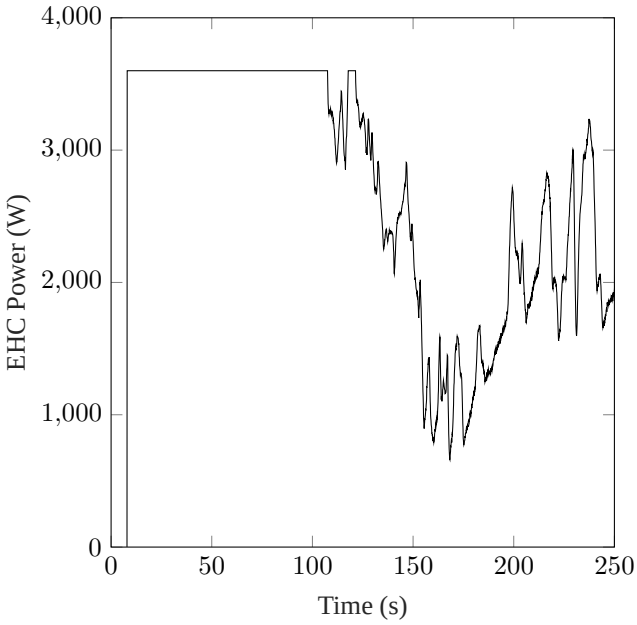

Figure 4. Heater power and limit.

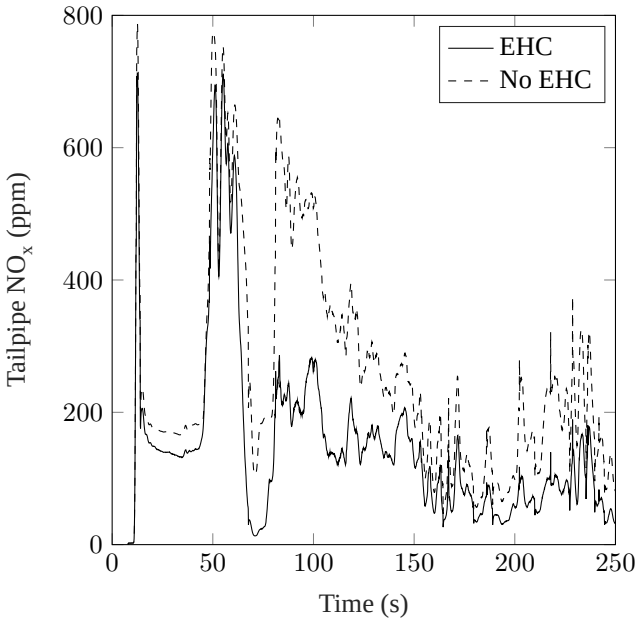

Figure 5. Tailpipe NO_x with SCR without and with heating element.

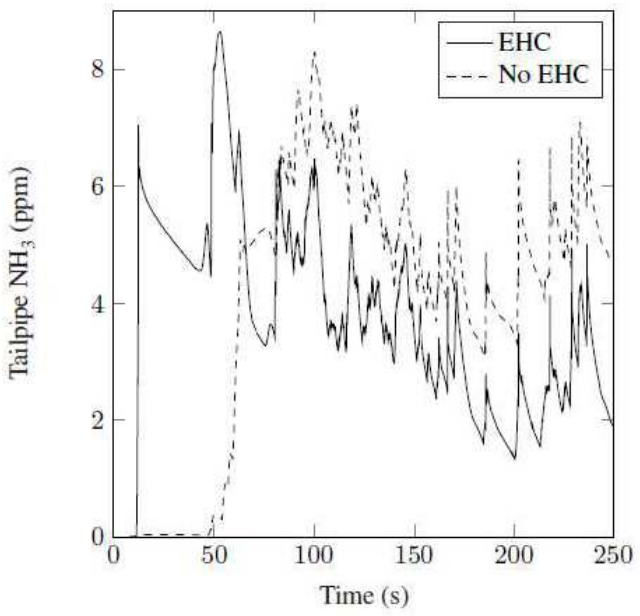

Figure 6. NH_3 slips with SCR without and with heating element.

Conclusions

Selective catalytic reduction has proven highly popular and effective in removal of NO_x from lean-burn direct injection engines. It presents significant challenges in terms of control, to optimally remove pollutants from the exhaust gas stream whilst respecting ammonia slip constraints. This results in a complex multi-layered control objective. We have demonstrated in this work that MPC works well in this respect. It systematically deals with constraints and provides a flexible cost function phrasing which permits expressing the desired tradeoff between ammonia slip and NO_x emissions, with a secondary objective of minimising consumption of urea and electrical energy. As a result, the benefits of MPC for control of an electrically heated SCR catalyst are numerous as compared with industry standard map-based control methods:

1. Tuning is much simpler, as the weights in (19) relate directly to the control objectives.
2. Systematic handling of constraints on the inputs and states mean that tuning the controller explicitly to respect constraints is not required.
3. Expansion of the aftertreatment control system to handle multiple-input, multiple-output structures, such as that presented in this work, is trivial, whereas interacting PID controller are significantly more difficult to tune.

Future work will be to achieve real-time operation of the controller developed in this work on embedded hardware suited to automotive applications. It would also be instructive to examine the possibility of extending the NMPC formulation to include adaptive MPC concepts in order to adapt to variation in the SCR plant over time, including ageing of the catalyst and calibration of the urea injector.

Acknowledgements

The authors thank Ricardo UK Ltd. for their sponsorship of this EngD project. The provision of EngD funding from EPSRC grant EP/G036896/1, the Industry Doctoral Training Centre in Transport and the Environment, and Royal Society grant RG140095 is gratefully acknowledged.

References

1. Committee on the Environment Effects of Air Pollution. Statement on the evidence for the effects of nitrogen dioxide on health. Department for Health, United Kingdom; 2014.
2. Hu Y, Chen Z, Zhao J, Chen H. ADRC based cascade controller design for urea selective catalytic reduction system. In: 2015 54th Annual Conference of the Society of Instrument and Control Engineers of Japan (SICE); 2015. p. 498–503.
3. Yuan X, Gao Y, Wang X. A novel NH_3 slip control for diesel engine selective catalytic reduction aftertreatment system. International Journal of Engine Research. 2016;17(2):169–178.
4. Lapuerta M, Ángel Ramos, Fernández-Rodríguez D, González-García I. High-pressure versus low-pressure exhaust gas recirculation in a Euro 6 diesel engine with lean-NOx trap: Effectiveness to reduce NOx emissions. International Journal of Engine Research. 2019;20(1):155–163.
5. Gosala DB, Ramesh AK, Allen CM, Joshi MC, Taylor AH, Voorhis MV, et al. Diesel engine aftertreatment warm-up through early exhaust valve opening and internal exhaust gas recirculation during idle operation. International Journal of Engine Research. 2018;19(7):758–773.
6. Willems F, Cloudt R, van den Eijnden E, van Genderen M, Verbeek R, de Jager B, et al. Is Closed-Loop SCR Control Required to Meet Future Emission Targets? In: SAE World Congress and Exhibition. SAE International; 2007. .
7. Song Q, Zhu G. Model-based Closed-loop Control of Urea SCR Exhaust Aftertreatment System for Diesel Engine. In: SAE 2002 World Congress and Exhibition. 2002-01-0287. SAE International; 2002. .
8. Schar CM, Onder CH, Geering HP. Control of an SCR catalytic converter system for a mobile heavy-duty application. IEEE Transactions on Control Systems Technology. 2006 July;14(4):641–653.
9. Ong CY, Annaswamy AM, Kolmanovsky IV, Laing P, Reed D. An Adaptive Proportional Integral Control of a Urea Selective Catalytic Reduction System based on System Identification Models. SAE International Journal of Fuels and Lubricants. 2010;3(1):625–642.
10. Upadhyay D, Nieuwstadt MV. Model Based Analysis and Control Design of a Urea-SCR deNOx Aftertreatment System. ASMEJournal of Dynamic Systems, Measurement, and Control. 2005;128(3):737–741.
11. Devarakonda M, Parker G, Johnson JH, Strots V. Model-based control system design in a urea-SCR aftertreatment system based on NH_3 sensor feedback. International Journal of Automotive Technology. 2009 Dec;10(6):653.
12. Sowman J, Laila DS, Cruden AJ, Fussey P. Nonlinear Model Predictive Control for Cold Start Selective Catalytic Reduction. IFAC-PapersOnLine. 2015;48(23):471–476. 5th IFAC Conference on Nonlinear Model Predictive Control NMPC 2015.

13. Zhang H, Wang J, Wang YY. Optimization of the ammonia coverage ratio references in diesel engine two-can selective catalytic reduction systems via nonlinear model predictive control. Proceedings of the Institution of Mechanical Engineers, Part D: Journal of Automobile Engineering. 2014;228(12):1452–1467.
14. McKinley TL, Alleyne AG. Model Predictive Control: A Unified Approach for Urea-Based SCR Systems. SAE International Journal of Fuels and Lubricants. 2010;3(1):673–689.
15. Chen P, Wang J. Coordinated Active Thermal Management and SCR Control for Simultaneous Fuel Economy Improvement and Emissions Reduction during Low-temperature Operations. Journal of Dynamic Systems, Measurement, and Control. 2015 07;137(12).
16. Safety, Accessibility and Sustainability Panel. Emissions from the TfL bus fleet. Transport for London, United Kingdom; 2015.
17. Nova I, Colombo M, Tronconi E. Kinetic Modeling of Dynamic Aspects of the Standard NH_3-SCR Reaction Over V_2O_5-WO_3/TiO_2 and Fe-Zeolite Commercial Catalysts for the Aftertreatment of Diesel Engines Exhausts. Oil & Gas Science and Technology. 2011 07;66:681–691.
18. Diehl M, Ferreau HJ, Haverbeke N. Efficient Numerical Methods for Nonlinear MPC and Moving Horizon Estimation. In: Magni L, Raimondo DM, Allgower F, editors. Nonlinear model predictive control, Towards New Challenging Applications. vol. 384 of Lecture Notes in Control and Information Sciences. Springer; 2009. p. 391–417.
19. Ferreau HJ, Bock HG, Diehl M. An online active set strategy to overcome the limitations of explicit MPC. International Journal of Robust and Nonlinear Control. 2008;18:816–830.